Inorganic Chemistry

Article

pubs.acs.org/IC

An Electrochemical and Spectroscopic Study of Nd(III) and Pr(III) Coordination in the 1-Butyl-1-methylpyrrolidinium Bis(trifluoromethylsulfonyl)imide Ionic Liquid Containing Chloride Ion

Li-Hsien Chou and Charles L. Hussey*

Department of Chemistry and Biochemistry, University of Mississippi, University, Mississippi 38677, United States

ABSTRACT: The coordination and accessible oxidation states of Nd and Pr were investigated in 1-butyl-1-methylpyrrolidinium bis(trifluoromethylsulfonyl)imide (BuMePyroTf_2N) by using electronic absorption spectroscopy, cyclic staircase voltammetry, and controlled potential coulometry. These experiments were carried out in the neat ionic liquid (IL) and in the IL containing free Cl^- from the dissolution of BuMePyroCl. The electrolytic dissolution of Ln = Nd and Pr metal in this IL produces only the respective Ln^{3+} ions. These trivalent species can be reduced to Ln^{2+}, but the resulting divalent species exhibit only transient stability, undergoing rapid disproportionation to Ln^{3+} and Ln^0. The intensity of the hypersensitive $^4G_{5/2} \leftarrow {}^4I_{9/2}$ electronic transition for Nd^{3+} dissolved in the IL was substantially larger than it was in noncoordinating solvents such as aqueous $HClO_4$, indicating moderate interactions between Nd^{3+} and Tf_2N^- ions, probably resulting in anionic species such as $[Nd(Tf_2N)_x]^{(x-3)-}$. The addition of Cl^- to $[Ln(Tf_2N)_x]^{(x-3)-}$ solutions results in the precipitation of $LnCl_3$(s) (s = solid). The $LnCl_3$(s) redissolves to give the octahedral complex $[LnCl_6]^{3-}$ as the Cl^- concentration is raised further. In the IL containing excess chloride, the $^3P_0 \leftarrow {}^3H_4$ transition for $[PrCl_6]^{3-}$ exhibits ligand-mediated pseudohypersensitive behavior.

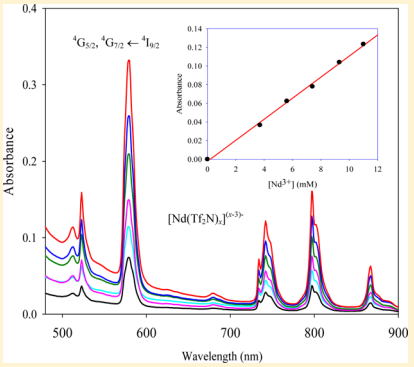

INTRODUCTION

Ionic liquids (ILs) are universally defined as organic salts that are molten below the boiling point of water.[1] The physical and chemical properties of second generation (nonchloroaluminate) ILs were nicely summarized in a recent article by K. E. Johnson.[2] There is considerable interest in exploiting these ILs as solvents in the nuclear fuel cycle (NFC), for example, for fission product separation and processing, where they would replace the inflammable volatile organic solvents (VOCs) currently used for this purpose. The prospects for utilizing ILs for these applications and some assessments of the research progress in this area have been discussed.[3−8] Spent nuclear fuel (SNF), that is, reactor fuel that can no longer sustain a nuclear chain reaction, contains primarily U and Pu; medium to long-lived fission products such as ^{137}Cs, ^{129}I, ^{90}Sr, and ^{99}Tc; isotopes of the minor actinides Am, Cm, and Np; and several lanthanides, including La, Ce, Pr, Nd, Sm, and Eu as well as radioactive Pm. The effective utilization of ILs for the processing of SNF, particularly for those processes incorporating redox chemistry, requires information about the solvation, redox potentials, stable oxidation states, and transport properties of the SNF components, especially f-block solutes, in these solvents. A particularly interesting approach to obtain this information is to use electrochemistry to probe the liquid−liquid interface during the extraction of fission products from water into hydrophobic ILs containing the ligands typically used for reprocessing SNF.[9−11] In addition to the processing of SNF, strategies are sought to recover rare earth materials from discarded electronic components and related high-tech waste by employing IL solvents, that is, by using these ionic solvents to carry out "urban mining."

Several reviews about the chemistry of f-block elements in ILs are available.[12−14] In previous papers, we reported the electrochemistry and electronic spectroscopy of Ce^{3+}, Eu^{3+}, Sm^{3+}, and Yb^{3+} in several bis(trifluoromethylsulfonyl)imide (Tf_2N^-)-based ILs.[15,16] These studies were focused on the coordination of these ions in the neat ILs as well as ILs containing Cl^- or the polydentate ligand, *N*,*N*,*N*′,*N*′-tetraoctyl-3-oxa-pentane diamide. These ionic solvents were chosen because of their stability against oxidation and reduction and their favorable spectroscopic windows. Although the chemistry of the lanthanide elements is limited for the most part to the trivalent species, we determined in these previous studies that it is possible to stabilize Ce^{4+} as $[CeCl_6]^{2-}$ and to obtain stable solutions of both Eu^{2+} and Yb^{2+} in the neat IL. However, like Ce^{3+}, the related trivalent species Sm^{3+}, Eu^{3+}, and Yb^{3+} form stable octahedral $[LnCl_6]^{3-}$ complexes, but the corresponding Ln^{4+} species, $[LnCl_6]^{2-}$, resulting from the oxidation of these three lanthanides, were not stable in the IL.

With the exception of an early attempt to investigate the electrochemistry of Nd^{3+} in mixtures of $AlCl_3$−BuPyCl and

Received: March 11, 2014
Published: May 14, 2014

   dx.doi.org/10.1021/ic5005616 | *Inorg. Chem.* 2014, 53, 5750−5758

$AlCl_3$−EtMeImCl,[17] prior investigations of the electrochemistry of Nd and Pr in molten salts/ILs, especially chloride-based systems, are restricted to a few investigations conducted in high-melting alkali chloride mixtures. For example, Castrilejo et al.[18] examined the reduction of Pr^{3+} to Pr at liquid Cd and Bi electrodes in LiCl−KCl. Yamana et al.[19] produced stable solutions of Nd^{2+} by reduction of dissolved $NdCl_3$ in this same molten salt at 773 K. However, the resulting Nd^{2+} did not exhibit long-term stability and slowly disproportionated to Nd^{3+} and Nd. The standard free energy change of the disproportionation reaction was ∼2 kJ mol^{-1}, which gives an equilibrium constant of about 4×10^{-2} for this reaction. In a series of two articles, Fukasawa et al.[20,21] reported the electrochemistry and spectroscopy of Nd^{3+} in molten alkali chloride and mixtures of alkali chlorides with alkali earth chlorides at 923 K. Notably, these authors described the effects of the chloride coordination environment on the hypersensitive 4f ← 4f transition, $^4G_{5/2} \leftarrow {}^4I_{9/2}$, which overlaps with the much weaker, nonhypersensitive $^2G_{7/2} \leftarrow {}^4I_{9/2}$ transition.[22] Mudring et al.[23] also examined this hypersensitive transition for NdI_3 dissolved in 1-dodecyl-3-methyimidazolium bis(trifluoromethylsulfonyl)imide. Fujii et al.[24] conducted a similar spectroscopic analysis of the octahedral $[PrCl_6]^{3-}$ complex in various molten alkali chlorides and examined the effects of the solvation environment on the oscillator strength for the hypersensitive $^3F_2 \leftarrow {}^3H_4$ transition in the near-infrared (NIR). As an extension of our previous work with trivalent Ce, Eu, Sm, and Yb, we report herein an investigation of the electrochemistry and electronic absorption spectroscopy of Nd^{3+} and Pr^{3+} in the BuMePyroTf_2N IL with and without added Cl^-. To our knowledge, no comprehensive investigation of the solvation and redox chemistry of these lanthanide elements has been carried out in ILs.

Because the number of 4f electrons for Nd and Pr falls between Ce and Sm, the findings of this investigation, taken with the results our previous work, should provide valuable insight into the periodic trends in the stability of the oxidation states of lanthanide species in Tf_2N-based ILs. In principle, both Nd and Pr are capable of attaining the tetravalent state, but only under special conditions such as in oxides or fluoride compounds.[25] The stability of these species in aqueous solutions is virtually nonexistent.

Most actinides and lanthanides are soluble in Tf_2N^--based ILs as a result of interactions between the f-block cations and the oxygen atoms of this anion.[26] In fact, a coordination number of 9−10 has been predicted for Eu^{3+} in BuMeImTf_2N on the basis of molecular dynamics simulations.[27] The homoleptic compounds BuMePyro$_2$[Ln(Tf_2N)$_5$], Ln = Nd^{3+}, Pr^{3+}, and Tb^{3+}, have been isolated from the BuMePyroTf_2N IL.[28,29] It is proposed that the lanthanide cations in these compounds are coordinated to nine oxygen atoms by one monodentate and four bidentate Tf_2N^- ligands. We have demonstrated in previous studies that Cl^- is a stronger ligand than Tf_2N^-.[15,16] In fact, the addition of Cl^- to solutions of $[Ln(Tf_2N)_x]^{(x-3)-}$ (Ln = Ce, Sm, Eu, and Yb) readily displaces Tf_2N^- from the solvation sphere of these ions. Thus, by analogy, the addition of Cl^- to solutions of Nd^{3+} and Pr^{3+} in BuMePyroTf_2N is expected to result in dramatic changes in the Nd^{3+} and Pr^{3+} coordination. These solvation changes should lead to changes in the voltammetry and electronic absorption spectroscopy of these ions. The presence of the hypersensitive transition for Nd^{3+} gives us a window into the coordination of this species in the IL. From our previous investigations with Ce, Sm, Eu, and Yb in Tf_2N-based ILs,[15,16] we know that the coordination of Ln^{3+} by Cl^- results in species that are thermodynamically more stable and thus easier to oxidize than Ln^{3+} solvated by Tf_2N^-. This fact may provide a strategy to access the elusive tetravalent Nd and Pr species in solution.

EXPERIMENTAL SECTION

The preparation, purification, and H_2O content of BuMePyroTf_2N and BuMePyroCl were described in a previous article.[30] Neodymium and praseodymium metals (Alfa AESAR, 99.98%) were used as obtained. Because f-block metals react readily with moisture and oxygen, it was necessary to carry out all experiments, except absorption spectroscopy, in a nitrogen-filled glovebox with H_2O and O_2 < 5 ppm. The electrochemical equipment used for this investigation and the application of electronic resistance compensation were described in previous articles.[15,16] The working electrode for voltammetric studies was a Teflon-shrouded platinum disk electrode with a geometrical surface area of 0.196 cm^2 (Pine Instruments Co.). The Bioanalytical Systems MF-2042 nonaqueous Ag^+/Ag reference electrode and membrane-isolated Pt counter electrode were the same as those used in previous investigations.[15,16] We determined experimentally that the potential of the Fc^+/Fc redox couple was +0.061 V versus the Ag/Ag^+ electrode. A small hot plate/stirrer was used to heat the electrochemical cell as needed. Using this arrangement, the temperature could be maintained to ±0.5 °C. The cells and instrumentation that were used to record electronic absorption spectra have been described.[15]

RESULTS AND DISCUSSION

Preparation of Ionic Liquid Solutions Containing Nd and Pr Ions. Solutions of Nd and Pr ions in BuMePyroTf_2N were prepared by the controlled potential electrolytic oxidation of the metals. A potential of 0.30 V versus Ag/Ag^+ was used for both Nd and Pr. The oxidation state n of the dissolved lanthanide ions was calculated from Faraday's law from the change in weight Δw of the Ln^0 electrode for a given anodic charge Q_a.

$$n = MQ_a/F\Delta w \quad (1)$$

In this expression, F is the Faraday constant, and the gram atomic mass of the lanthanide is represented by M. The data in Table 1 indicate that Nd^{3+} and Pr^{3+} are the species produced in these experiments. As noted in previous work, this coulometric method for preparing Ln^{3+} solutions is advantageous because it circumvents the dissolution of salts or complexes with anions different from Tf_2N^-. With the IL being very dry (<2 ppm of H_2O), the resulting lanthanide ions can only be solvated by this anion. The interactions of Nd^{3+} and Pr^{3+} with Tf_2N^- were probed with electronic absorption spectroscopy.

Table 1. Anodic Dissolution of Nd and Pr Metal Electrodes in BuMePyroTf_2N at 0.30 V

	Δw (g)	Q_a (C)	n
Nd	0.0196	40.0	3.05
	0.0147	30.2	3.06
	0.0181	36.7	3.03
Pr	0.0170	35.6	3.04
	0.0157	32.5	3.00
	0.0170	36.0	3.09

Electronic Absorption Spectroscopy of Nd^{3+} and Pr^{3+} in BuMePyroTf_2N. Absorption spectra for solutions of Nd^{3+} ($4f^3$) and Pr^{3+} ($4f^2$) in BuMePyroTf_2N at different concentrations are shown in Figures 1 and 2, respectively. The spectra of Nd^{3+} in Figure 1 exhibit several low-intensity absorption

dx.doi.org/10.1021/ic5005616 | Inorg. Chem. 2014, 53, 5750−5758

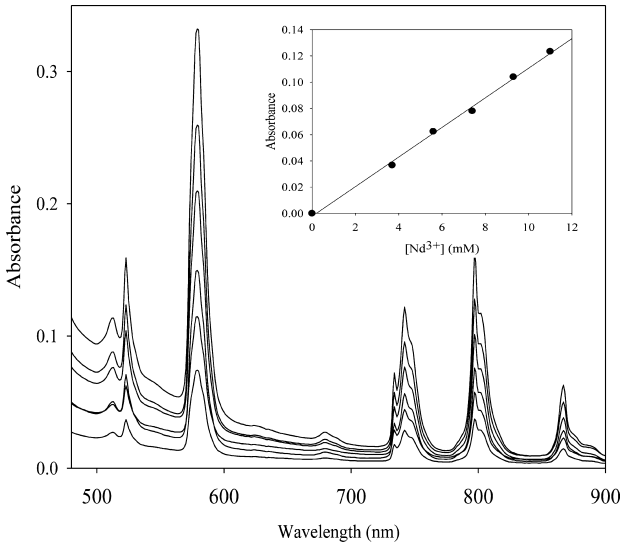

Figure 1. Electronic absorption spectra of Nd^{3+} in $BuMePyroTf_2N$ at different concentrations. (inset) Absorbance at 579 nm as a function of the Nd^{3+} concentration.

bands at 511 nm, 523 nm (6 L mol^{-1} cm^{-1}), 579 nm (20 L mol^{-1} cm^{-1}), 697 nm, 741 nm (7 L mol^{-1} cm^{-1}), 797 nm (10 L mol^{-1} cm^{-1}), and 866 nm (4 L mol^{-1} cm^{-1}) as well as shoulders at 733, 748, and 801 nm. It is well-established that these sharp but weak bands arise from various Laporte-forbidden intraconfigurational 4f ← 4f electronic transitions. The electronic transitions corresponding to these bands are nicely summarized by Binnemans and Görller-Walrand.[31]

The inset of Figure 1, which was constructed with data from the most intense band at 579 nm, verifies that the spectrum of Nd^{3+} obeys the Lambert−Beer law in this solvent. With only one exception, the IL spectra in Figure 1 are remarkably similar to those found in aqueous 1.0 M $HClO_4$.[31,32] This is not completely unexpected because as a general rule the solvation environment has little influence on most of the 4f ← 4f electronic transitions observed for Ln^{3+} ions. However, the 579 nm band is a notable exception. This band, which arises from overlap of the hypersensitive $^4G_{5/2}$ ← $^4I_{9/2}$ and non-hypersensitive $^2G_{7/2}$ ← $^4I_{9/2}$ transitions, is commonly used to probe the coordination of Nd^{3+} ions in solution because the intensity generally increases and shape of the band often changes with an increase in complexation.[33] As a first approximation, the influence of the IL solvation environment can be assessed by comparing the intensity of this band to the intensities of some other 4f ← 4f electronic transitions in the Nd^{3+} spectrum that are known to be largely unaffected by solvent interactions, for example, the $^2H_{9/2}$ ← $^4I_{9/2}$ transition at 797 nm. In aqueous $HClO_4$ solutions, where minimal interactions between Nd^{3+} and the solvent are to be expected, the intensity ratio ε_{579}:ε_{797} for these two transitions is about 1:2,[34] whereas in aqueous solutions of Nd^{3+} containing ethylenediaminetetraacetic acid, this ratio approaches ∼1:1.[35] For the spectra in Figure 1, the ratio is ∼1.9:1. This ratio is significantly larger than that found in the aqueous $HClO_4$ solutions and in related ILs with relatively noncoordinating anions, including 1-ethyl-3-methylimidazolium triflate (1:1).[36] These findings are in accord with the results of our recent investigation of the Eu^{3+} hypersensitive $^5D_2$ ← $^7F_0$ transition in $BuMe_3NTf_2N$.[16]

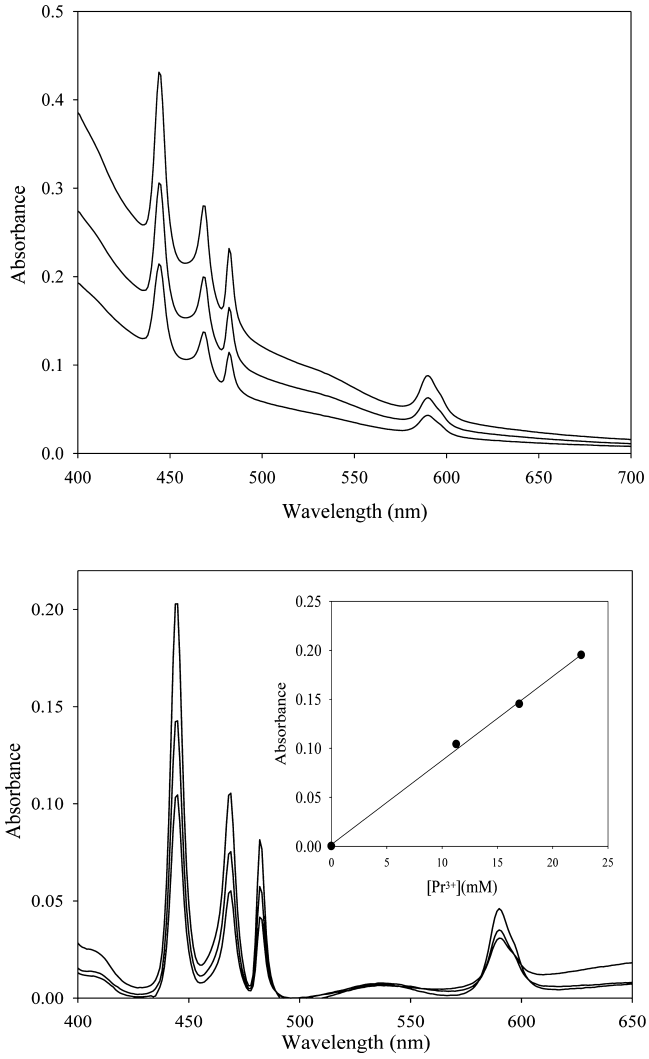

Figure 2. Electronic absorption spectra of Pr^{3+} in $BuMePyroTf_2N$ at different concentrations before (top) and after (bottom) background correction. (inset) Absorbance at 440 nm as a function of the Pr^{3+} concentration.

Figure 2 (top) shows absorption spectra for solutions of Pr^{3+} in $BuMePyroTf_2N$ at different concentrations. Because the 4f ← 4f transitions for Pr^{3+} exhibit low intensity, it was necessary to prepare fairly concentrated solutions. At high concentrations, the resulting spectra display a strongly increasing baseline with decreasing wavelength consistent with Rayleigh scattering. This phenomenon, which is absent from the neat IL, was also noted during a previous investigation of Eu^{3+}, Sm^{3+}, and Yb^{3+},[16] and complicates efforts to record quality spectra for lanthanide species in this IL that exhibit low-intensity absorption bands. (This problem is also apparent for Nd^{3+} (Figure 1), but the bands of interest appear at somewhat higher wavelengths than they do for Pr^{3+}. No baseline corrections were deemed necessary.) As noted previously, we suspect that this scattering arises from small particles of silica or oxide impurities that are present in the lanthanide metals and released into the solution during oxidation. Fortunately, we have developed a simple, effective digital procedure for correcting the spectral baseline in such cases.[16] This procedure was applied to the spectra in Figure 2, and the resulting corrected spectra are shown in the bottom panel.

dx.doi.org/10.1021/ic5005616 | Inorg. Chem. 2014, 53, 5750−5758

The spectrum of Pr^{3+} recorded in the IL consists of four low-intensity bands at 445 nm (8.4 L mol^{-1} cm^{-1}), 469 nm (4.4 L mol^{-1} cm^{-1}), 482 nm (3.3 L mol^{-1} cm^{-1}), and 590 nm (1.8 L mol^{-1} cm^{-1}). The first group of three bands is attributed to the spin-allowed transitions $^3P_2 \leftarrow {}^3H_4$, $^3P_1 \leftarrow {}^3H_4$, and $^3P_0 \leftarrow {}^3H_4$, respectively, and the band at 590 nm arises from the $^1D_2 \leftarrow {}^3H_4$ transition. As was the case for Nd^{3+}, these spectra are quite similar to their counterparts in aqueous $HClO_4$.[31,32] (Note: the weak broad band at around 540 nm is believed to be an artifact of the correction process or a small amount of an impurity in the IL because no transitions are known to occur at this wavelength/energy.) The inset of Figure 2, which was prepared from data for the most intense band at 445 nm ($^3P_1 \leftarrow {}^3H_4$), shows that the Pr^{3+} spectrum obeys the Lambert–Beer law. Like Nd^{3+}, Pr^{3+} is reported to display a hypersensitive transition, which in this case is attributed to the $^3F_2 \leftarrow {}^3H_4$ transition.[33] Unfortunately, the absorption band for this process is located at ~1920 nm and is outside the range of our instrumentation.

Overall, the results presented above for Nd^{3+}, as well as those resulting from a recent investigation of Eu^{3+},[16] suggest moderate interactions between trivalent lanthanide ions and Tf_2N^-. Isolation of the homoleptic crystalline compounds $[BuMePyro]_2[Nd(Tf_2N)_5]$[28] and $[BuMePyro]_2[Pr(Tf_2N)_5]$[29] seems to support this result. Although the exact coordination number of lanthanide ions in Tf_2N-based IL solutions is not completely clear and may be as great as 9–10,[23] interactions between these anions and Ln^{3+} species would be expected to result in anionic complexes of the type $[Ln(Tf_2N)_x]^{(x-3)-}$.

Cyclic Voltammetry of Nd^{3+} and Pr^{3+} in BuMePyro-Tf_2N. Figures 3 and 4 show voltammograms acquired at a Pt electrode in BuMePyroTf_2N after the coulometric addition of various amounts of Nd^{3+} and Pr^{3+}, respectively. The top frames in both figures show that individual solutions of these ions exhibit one well-defined reduction wave and at least one oxidation wave. The insets in these frames verify that the reduction waves scale linearly with the ion concentrations at a fixed scan rate. No additional reduction waves were observed for either species prior to the negative potential limit of the IL. The voltammograms for Nd^{3+} and Pr^{3+} exhibit oxidation waves immediately following scan reversal that appear to be associated with the reduction waves. These waves are more prominent for the Nd^{3+} reduction product (Figure 3) than they are for the species resulting from the reduction of Pr^{3+} (Figure 4). These voltammograms are very similar in appearance to those recorded during the reduction of trivalent lanthanides that can be reduced to stable divalent species in Tf_2N^--based ILs,[16,37−39] notably Eu^{3+}, Sm^{3+}, and Yb^{3+}. This correspondence provides good evidence that these oxidation waves most likely arise from Nd^{2+} and Pr^{2+} produced in the electrode diffusion layer. However, the small scan rate-dependent oxidation currents associated with these waves indicate that these divalent species exhibit only limited stability.

The bottom panels in Figures 3 and 4 show voltammograms recorded at different scan rates at fixed concentrations of Nd^{3+} and Pr^{3+}, respectively. Table 2 shows data taken from these voltammograms. They reveal that the cathodic peak potentials E_p^c for the Nd^{3+} and Pr^{3+} reduction waves are quite similar in value and vary with the scan rate, shifting to more negative potentials as the scan rate is increased. In addition, these data reveal that the peak current functions $i_p^c/\nu^{1/2}$, where ν is the scan rate, for these waves decrease by 37 and 32% as the scan rates are increased from 0.010 to 0.30 V s^{-1}, respectively,

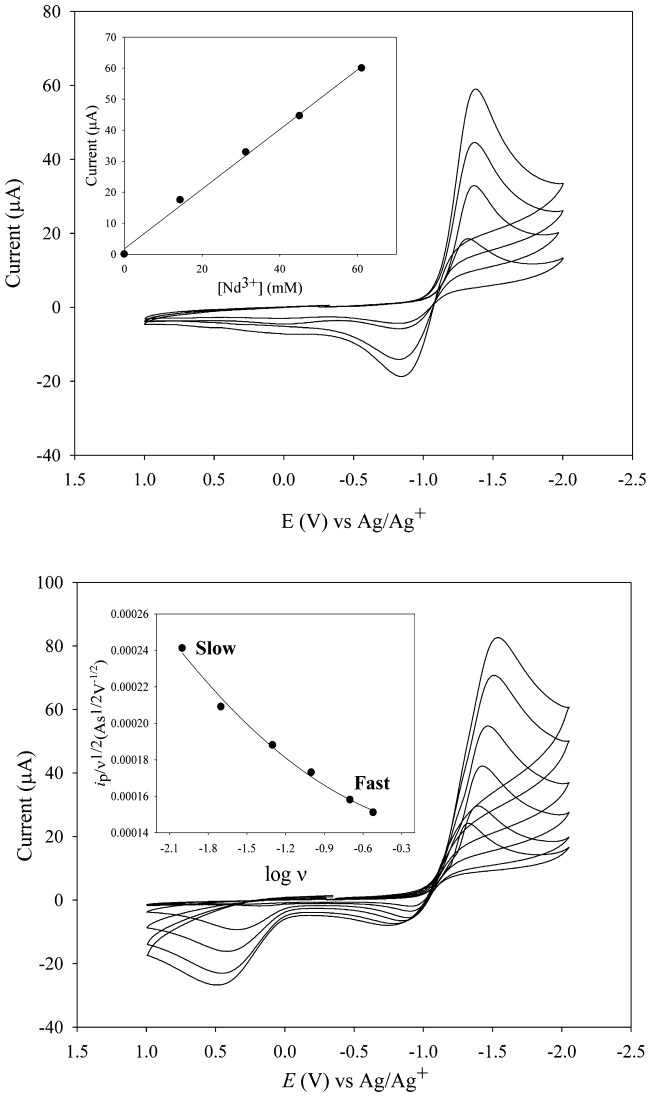

Figure 3. Cyclic staircase voltammograms acquired at a Pt electrode in BuMePyroTf_2N. (top) 0.014, 0.031, 0.045, and 0.061 M Nd^{3+}; the scan rates were 50 mV s^{-1}. (inset) Plot of the reduction peak current versus the Nd^{3+} concentration. (bottom) Voltammograms recorded at a Pt electrode in BuMePyroTf_2N containing 0.061 M Nd^{3+} as a function of scan rate. (inset) Peak current function versus the logarithm of the scan rate.

signaling that both reactions are complicated by coupled homogeneous chemical reactions. Furthermore, in concordance with the voltammetric results, it was not possible to prepare solutions of Nd^{2+} or Pr^{2+} by the exhaustive bulk electrolysis of solutions containing the trivalent species. Our many attempts to reduce the trivalent species directly to Nd^0 or Pr^0 produced an intractable, insulating electrode surface film before a substantial amount of the respective trivalent species could be reduced. These results are consistent with a charge-transfer reaction with a coupled homogeneous chemical step in which Ln^{2+} produced by reduction of the parent trivalent species rapidly disproportionates to Ln^{3+} and Ln^0.

$$Ln^{3+} + e^- \rightleftharpoons Ln^{2+} \quad (1)$$

$$3Ln^{2+} \rightarrow 2Ln^{3+} + Ln^0 \quad (2)$$

The Ln^0 thus produced reacts with the components of the IL, probably resulting in decomposition of the Tf_2N^- anion

dx.doi.org/10.1021/ic5005616 | Inorg. Chem. 2014, 53, 5750−5758

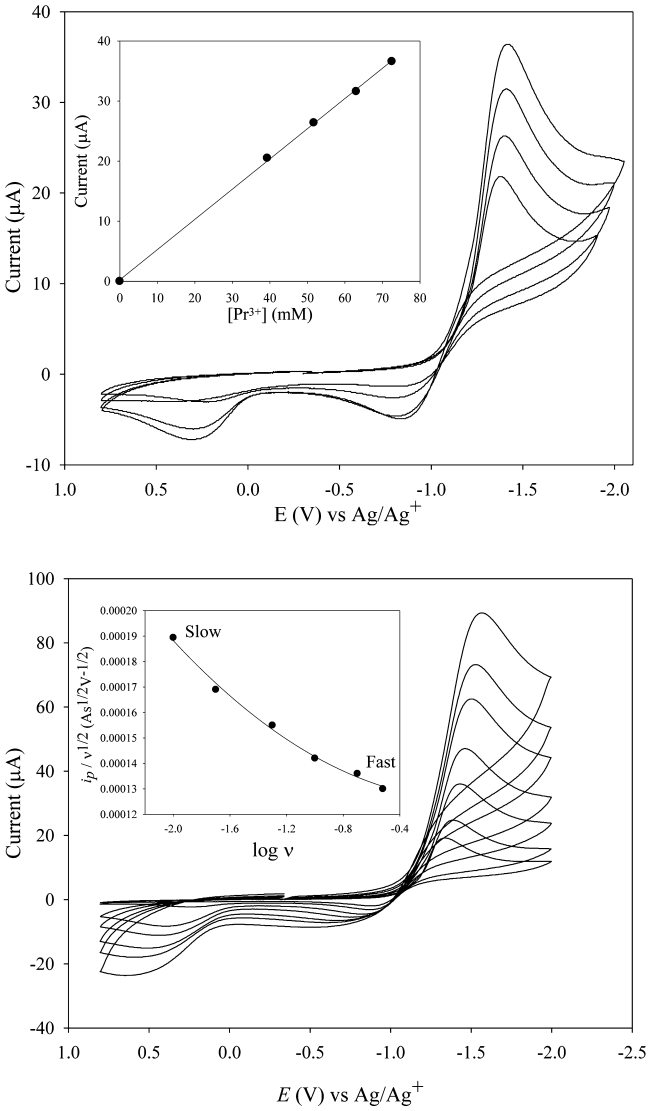

Figure 4. Cyclic staircase voltammograms recorded at a Pt electrode in $BuMePyroTf_2N$. (top) 0.039, 0.052, 0.063, and 0.073 M Pr^{3+}; the scan rates were 50 mV s^{-1}. (inset) Plot of the reduction peak current versus the Pr^{3+} concentration. (bottom) Voltammograms recorded at a Pt electrode in $BuMePyroTf_2N$ containing 0.073 M Pr^{3+} as a function of scan rate. (inset) Peak current function versus the logarithm of the scan rate.

through a reaction with Ln^0 to form a passivating film on the electrode surface. Similar results were reported during the attempted electrodeposition of other active metals such as Li in Tf_2N-based ILs.[40−43] Furthermore, these results are the same as those observed during the reduction of Ce^{3+} in $BuMePyroTf_2N$.[15] They are consistent with the rarity of stable Nd^{2+} and Pr^{2+} species in solution and in coordination compounds, and with the known tendency of these divalent species to disproportionate.[21]

Amperometric Titration: Addition of Cl^- to Nd^{3+} and Pr^{3+} Solutions. Amperometric titration experiments were used to investigate the coordination of Ln^{3+} ions by chloride. In these experiments, the voltammetric oxidation and reduction currents for Nd^{3+} and Pr^{3+} were recorded in IL solutions containing fixed amounts of each ion after the addition of Cl^- as BuMePyroCl. The top panels of Figures 5 and 6 show some of the voltammograms that resulted from titration experiments with Nd^{3+} and Pr^{3+}, respectively. The plots given in the bottom panels of these figures provide graphical summaries of the results. For Nd^{3+}, the plots in Figure 5 give the reduction current at E_p^c = −1.37 V (left-hand axis) and the oxidation current at E_p^a = 1.30 V (right-hand axis) as a function of the molar ratio of Cl^- to Nd^{3+}, mCl^-/mNd^{3+}. Similar results for Pr^{3+} are given in Figure 6 (bottom panel) as plots of the reduction current at E_p^c = −1.40 V (left-hand axis) and oxidation current at E_p^a = 1.40 V (right-hand axis) versus mCl^-/mPr^{3+}. (Note that no oxidation currents can be observed for either trivalent species until a certain amount of Cl^- is present in the solutions *vide infra*.)

After the first small addition of Cl^-, the Nd^{3+} and Pr^{3+} reduction currents increased by a small amount, and the peak current ratio i_p^a/i_p^c for the $Nd^{3+/2+}$ reaction decreased further. This ratio could not be measured for the $Pr^{3+/2+}$ reaction because there was little or no current associated with the reverse scans. This behavior is very similar to that reported for the reduction of Ce^{3+} under similar conditions and was ascribed to chloride-induced promotion of the rate of the Ce^{2+} disproportionation reaction.[15] The addition of more Cl^- has no significant effect on the peak currents for the Nd^{3+} and Pr^{3+} reduction waves until $mCl^-/mNd^{3+} \approx 3$. At this induction point, finely divided white solids became apparent in both solutions, and the Nd^{3+} and Pr^{3+} reduction currents decreased by about 50%, indicating the loss of about one-half of these trivalent species from the solutions. We did not attempt to recover these precipitates and subject them to elemental analysis. However, during a similar investigation involving Ce^{3+},

Table 2. Cyclic Staircase Voltammetric Data in $BuMePyroTf_2N$

	ν (V s^{-1})	log ν	E_p^c (V)	$10^5 i_p$ (A)	$10^4 i_p/\nu^{1/2}$ (A $s^{1/2}$ $V^{-1/2}$)
$Nd^{3+/2+}$	0.01	−2.00	−1.324	2.41	2.41
	0.02	−1.70	−1.396	2.96	2.09
	0.05	−1.30	−1.424	4.42	1.88
	0.10	−1.00	−1.464	5.48	1.73
	0.20	−0.70	−1.506	7.07	1.58
	0.30	−0.52	−1.538	8.26	1.51
$Pr^{3+/2+}$	0.01	−2.00	−1.354	1.91	1.90
	0.02	−1.70	−1.388	2.47	1.69
	0.05	−1.30	−1.430	3.61	1.55
	0.10	−1.00	−1.458	4.71	1.42
	0.20	−0.70	−1.500	6.25	1.36
	0.30	−0.52	−1.532	7.32	1.30

dx.doi.org/10.1021/ic5005616 | *Inorg. Chem.* 2014, 53, 5750−5758

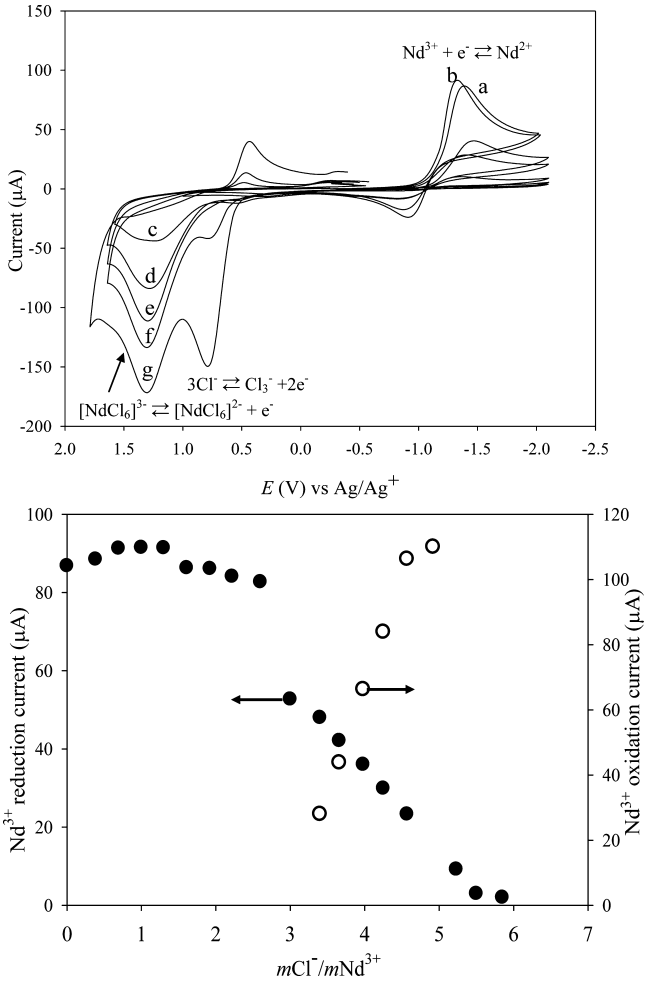

Figure 5. (top) Examples of cyclic staircase voltammograms acquired at a Pt electrode in BuMePyroTf$_2$N containing: (a) 0.061 M Nd^{3+}, (b) 0.061 M Nd^{3+} + 0.067 M Cl^- (mCl^-/mNd^{3+} = 1.1), (c) 0.061 M Nd^{3+} + 0.23 M Cl^- (mCl^-/mNd^{3+} = 3.8), (d) 0.061 M Nd^{3+} + 0.26 M Cl^- (mCl^-/mNd^{3+} = 4.3), (e) 0.061 M Nd^{3+} + 0.31 M Cl^- (mCl^-/mNd^{3+} = 5.1), (f) 0.061 M Nd^{3+} + 0.34 M Cl^- (mCl^-/mNd^{3+} = 5.6), and (g) 0.061 M Nd^{3+} + unbound excess Cl^- (mCl^-/mNd^{3+} > 6). The scan rates were 50 mV s^{-1}. (bottom) Plots of the Nd^{3+} voltammetric reduction and oxidation currents versus mCl^-/mNd^{3+} following the addition of Cl^- to a 0.061 M solution of Nd^{3+} in BuMePyroTf$_2$N.

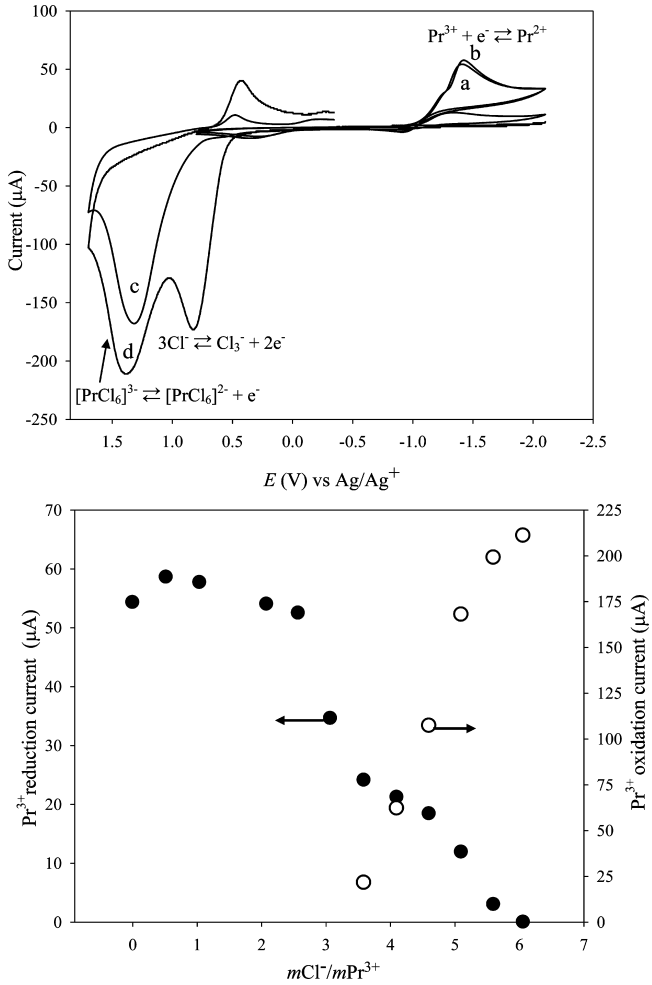

Figure 6. (top) Examples of cyclic staircase voltammograms acquired at a Pt electrode in BuMePyroTf$_2$N containing: (a) 0.073 M Pr^{3+}, (b) 0.073 M Pr^{3+} + 0.075 M Cl^- (mCl^-/mPr^{3+} = 1.0), (c) 0.073 M Pr^{3+}+ 0.37 M Cl^- (mCl^-/mPr^{3+} = 5.1), and (d) 0.073 M Pr^{3+} + unbound excess Cl^- (mCl^-/mPr^{3+} > 6). The scan rates were 50 mV s^{-1}. (bottom) Plots of the Pr^{3+} voltammetric reduction and oxidation currents versus mCl^-/mPr^{3+} following the addition of Cl^- to a 0.073 M solution of Pr^{3+} in BuMePyroTf$_2$N.

elemental analysis revealed that the precipitate was composed mainly of $CeCl_3$ with small quantities of entrapped IL residue, H_2O (from the aqueous work-up), and Ce_xO_y.[15] Thus, in all likelihood, the precipitates observed for Nd^{3+} and Pr^{3+} are the trivalent chloride compounds $NdCl_3$ and $PrCl_3$, respectively. However, these precipitates are not observed in the IL until the chloride concentration is sufficient to exceed the solubility products K_{sp} = $[Ln^{3+}][Cl^-]^3$ of the respective compounds. Estimation of K_{sp} from $[Ln^{3+}]$ and $[Cl^-]$ at the point where the first sudden decrease in the voltammetric current for Ln^{3+} reduction is observed gave 2.4×10^{-4} for $NdCl_3$ and 5.4×10^{-4} for $PrCl_3$. Similar data from a previous investigation of Ce^{3+} gave $K_{sp} = 2.6 \times 10^{-3}$ for $CeCl_3$.

The Nd^{3+} and Pr^{3+} reduction currents continue to decrease after each addition of Cl^- until mCl^-/mNd^{3+} and mCl^-/mPr^{3+} reach ~6. At this ratio, the solutions become completely clear, and the precipitate is gone. The voltammograms assigned to the $Nd^{3+/2+}$ and $Pr^{3+/2+}$ electrode reactions are no longer evident. Relatedly, when these ratios exceed 3, new oxidation waves are apparent at E_p^a = 1.30 and 1.40 V in the top panels of Figures 5 and Figure 6, respectively. These very positive voltammetric waves are assigned to the $Ln^{3+/4+}$ reaction. Thus, as a result of the increased thermodynamic stability afforded to Nd^{3+} and Pr^{3+} by complexation with chloride, the potentials of the $Ln^{3+/4+}$ and $Ln^{3+/2+}$ reactions shift toward more negative values. As a result, the oxidation of both Nd^{3+} and Pr^{3+} can be accessed at potentials slightly less positive than that leading to oxidation of the IL, whereas the reduction of these ions now appears to lie below the IL negative potential limit. Unfortunately, none of these voltammograms exhibit reverse currents, indicating that unlike Ce^{4+}, both Nd^{4+} and Pr^{4+} are chemically unstable in this IL. The currents for the two $Ln^{3+/4+}$ oxidation waves shown in the bottom panels of Figures 5 and 6 continue to rise after each addition of Cl^- until both mCl^-/mNd^{3+} and mCl^-/mPr^{3+} exceed ~5, after which they begin to level off. When these ratios exceed 6, a new oxidation wave can be detected in the solution at $E_p^a \approx 0.90$ V (Figures 5 and 6, upper panels). This wave is located at the same peak potential in both solutions. The peak current for this wave continues to

dx.doi.org/10.1021/ic5005616 | Inorg. Chem. 2014, 53, 5750−5758

grow as $m\mathrm{Cl}^-/m\mathrm{Ln}^{3+}$ is increased. Compton et al.[44,45] assigned this wave to the oxidation of chloride according to the following reaction (eq 3). The current for this wave directly reflects the Cl^- that is not coordinately bound to the trivalent lanthanide ions.

$$3\mathrm{Cl}^- \rightleftharpoons \mathrm{Cl}_3^- + 2\mathrm{e}^- \quad (3)$$

Amperometric Titration: Addition of Nd^{3+} and Pr^{3+} to Solutions of Cl^-. A second type of amperometric titration experiment was devised for the purpose of probing the coordination of Nd^{3+} and Pr^{3+} in solutions containing Cl^-. These experiments were similar to those used in previous investigations to assess the chloride coordination of Ce^{3+}[15] as well as Eu^{3+}, Sm^{3+}, and Yb^{3+}.[16] In these experiments, controlled potential coulometry was employed to introduce measured amounts of each Ln^{3+} species into solutions already containing known, fixed amounts of Cl^-. The progress of these experiments was followed by using voltammetry to monitor the Cl^- oxidation current, and hence the Cl^- concentration in the IL following each addition of Ln^{3+}. (During previous experiments with Ce^{3+}, we established that the Cl^- oxidation current varied linearly with its concentration.[15]) Figure 7 (top panel) shows voltammograms acquired after the electrolytic addition of different amounts of Nd^{3+}, whereas the bottom panel shows similar experiments involving Pr^{3+}. As the concentrations of Nd^{3+} and Pr^{3+} in these solutions increase, the oxidation wave for Cl^- decreases. Because the oxidation waves for the $Nd^{3+/4+}$ and $Pr^{3+/4+}$ reactions are very small and appear on the positive potential side of the current tail for the Cl^-/Cl_3^- reaction, it was not possible to obtain any useful information by monitoring these waves. Plots of the Cl^- oxidation currents as a function of the Nd^{3+} and Pr^{3+} concentrations are given in the insets of Figure 7. The average slope of these two plots is 6.0 ± 0.1, indicating that both Nd^{3+} and Pr^{3+} form six-coordinate, octahedral chloride complexes $[LnCl_6]^{3-}$.

Absorption Spectra of Nd^{3+} and Pr^{3+} in a Chloride Coordination Environment. The result that both Nd^{3+} and Pr^{3+} form six-coordinate chloride complexes in IL solutions containing excess chloride presents the opportunity to compare the resulting spectra of these solutions with those in Figures 1 and 2 that were recorded for these same species solvated only by Tf_2N^- ions. An absorption spectrum of Nd^{3+} in $BuMePyroTf_2N$ containing excess chloride ($m\mathrm{Cl}^-/m\mathrm{Nd}^{3+}$ = 7) is shown in Figure 8. This spectrum exhibits several bands that are obvious counterparts of those seen in Figure 1, but there are some notable differences as well. For example, the bands that are apparent at 741, 797, and 866 nm in Figure 1 are also present in Figure 8 but are slightly red-shifted to 749, 806, and 872 nm. The bands seen at 511 and 523 nm in Figure 1 are also present in Figure 8 but are greatly reduced in intensity. However, what is most significant is that the band attributed to the degenerate $^4G_{5/2}$, $^4G_{7/2} \leftarrow {}^4I_{9/2}$ transition, which appears as a single more or less symmetrical peak located at 579 nm in Figure 1, is now resolved into four bands appearing at 578, 588, 596, and 607 nm in the IL containing Cl^- (Figure 8, inset). The overall appearance of this spectrum is very similar to that seen for $[NdCl_6]^{3-}$ in both molten NaCl–2CsCl at 1023 K[19] and 2LiCl–3CsCl at 973 K.[20] The presence of these four bands in these high-temperature melts is attributed to splitting of the degenerate energy states for the $^4G_{5/2}$, $^4G_{7/2} \leftarrow {}^4I_{9/2}$ transition and indicates that $[NdCl_6]^{3-}$ exists in a highly symmetrical octahedral coordination.[20,22] Conversely, the single band seen

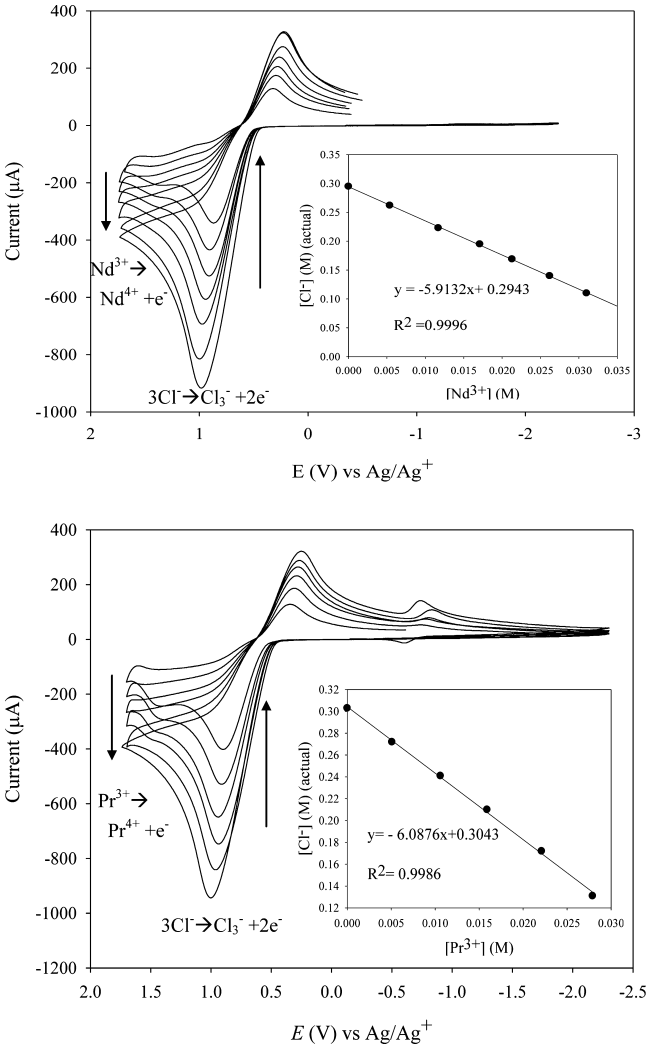

Figure 7. Cyclic staircase voltammograms recorded at a Pt electrode in 0.30 M solutions of BuMePyroCl in $BuMePyroTf_2N$ as a function of the (top) Nd^{3+} and (bottom) Pr^{3+} concentrations. (insets) Plots of the Cl^- concentrations determined from CSV versus the respective Ln^{3+} concentrations. The scan rates were 50 mVs^{-1}.

for $[NdCl_6]^{3-}$ in molten $CaCl_2$ and LiCl is attributed to distortion of the octahedral symmetry of this complex.

Figure 9 shows an absorption spectrum of Pr^{3+} in $BuMePyroTf_2N$ containing excess chloride ($m\mathrm{Cl}^-/m\mathrm{Pr}^{3+}$ = 9). Comparison of this spectrum with those in Figure 2 reveals similar low-intensity bands attributed to the $^3P_2 \leftarrow {}^3H_4$, $^3P_1 \leftarrow {}^3H_4$, and $^3P_0 \leftarrow {}^3H_4$ transitions as well as the band arising from the $^1D_2 \leftarrow {}^3H_4$ transition. However, as was the case for Nd^{3+}, these 4f ← 4f transitions are red-shifted and now appear at 450, 474, 486, and 596 nm, respectively. One notable difference between these two sets of spectra is the unexpected enhanced intensity of the $^3P_0 \leftarrow {}^3H_4$ band in the chloride-rich solution (Figure 9) compared to the neat IL. By comparison, the intensities of the $^3P_2 \leftarrow {}^3H_4$ and $^3P_1 \leftarrow {}^3H_4$ transitions retain the same mutual proportionality found in the neat IL. Like Nd^{3+}, the electronic spectra of Pr^{3+} have been investigated in molten alkali and alkaline-earth chloride salts. Fujii et al.[24] investigated the electronic spectra of Pr^{3+} in molten $CaCl_2$, LiCl, 3LiCl–2KCl, and NaCl–2CsCl. The aggregate of the cations in these molten salts displays a range of polarizabilities, which leads to different electron-donating abilities for Cl^- in

dx.doi.org/10.1021/ic5005616 | Inorg. Chem. 2014, 53, 5750–5758

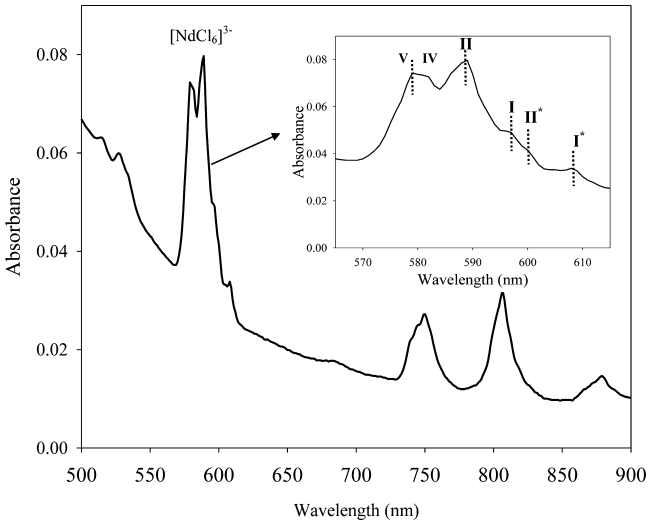

Figure 8. Electronic absorption spectrum of Nd^{3+} recorded in BuMePyroCl + BuMePyroTf_2N with $mCl^-/mNd^{3+} \approx 7$. (inset) Band assignments based on ref 17.

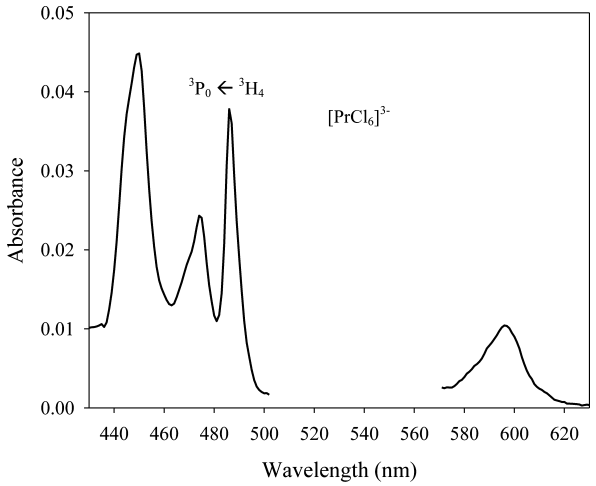

Figure 9. Electronic absorption spectrum of Pr^{3+} recorded in BuMePyroCl + BuMePyroTf_2N with $mCl^-/mPr^{3+} \approx 9$. (Artifacts resulting from the background correction procedure were removed from the spectrum in the 505 to 565 nm wavelength region.)

each salt or mixture. In their work, they noted that the $^3P_0 \leftarrow {}^3H_4$ band, which is not known to exhibit classical hypersensitivity, was split into two closely spaced peaks in mixtures of NaCl−2CsCl at 923 K, the molten salt with the greatest donating ability. This result was attributed to the undistorted octahedral symmetry of the $[PrCl_6]^{3-}$.

We did not detect any splitting of the $^3P_0 \leftarrow {}^3H_4$ band in the IL, only an increase in intensity. Because the enhanced intensity of this band is only observed in the IL after complexation with Cl^-, we ascribe it to ligand-mediated pseudohypersensitivity.[42] In fact, the pseudohypersensitivity of this particular transition is well-known and is used routinely to probe the complexation of Pr^{3+} with various biomolecules.[46,47]

SUMMARY

The electrochemistry and absorption spectroscopy of Nd^{3+} and Pr^{3+} were investigated in BuMePyroTf_2N with and without added Cl^-. In the neat IL, the electronic absorption spectra of both species were very similar to those recorded in aqueous $HClO_4$, with the exception of the band corresponding to the degenerate hypersensitive $^4G_{5/2}$, $^4G_{7/2} \leftarrow {}^4I_{9/2}$ transition for Nd^{3+}. This transition was more intense, suggesting significant interactions between Nd^{3+} and Tf_2N^- anions. Voltammetric experiments indicated that both trivalent species could be reduced within the potential window of the neat IL. However, these electrode reactions appear to be complicated by homogeneous chemistry, and any Ln^{2+} produced during these reduction reactions disproportionates rapidly to Ln^{3+} and Ln^0 with the latter reacting with the IL to form an insulating passive film on the electrode surface. Amperometric titration experiments in which Cl^- was added to solutions of Nd^{3+} and Pr^{3+} in BuMePyroTf_2N revealed the following sequence of reactions

$$[Ln(Tf_2N)_x]^{(x-3)-} + 3Cl^- \rightleftharpoons LnCl_3(s) + xTf_2N^- \quad (4)$$

$$LnCl_3(s) + 3Cl^- \rightleftharpoons [LnCl_6]^{3-} \quad (5)$$

where $[Ln(Tf_2N)_x]^{(x-3)-}$ precipitates as $LnCl_3(s)$ and then redissolves as the octahedrally coordinated $[LnCl_6]^{3-}$ complex. Thus, Nd^{3+} and Pr^{3+} as well as Ce^{3+} are classic examples of metal ions that form sparingly soluble salts with a particular anion, in this case Cl^-, and then increase in solubility through the formation of a complex with an excess of the anion, leading to a solubility minimum.[48] This is the first observation of such behavior in ILs, but it may be more common than has been realized.

The $[LnCl_6]^{3-}$ complexes can be oxidized to the respective Ln^{4+} species, presumably $[LnCl_6]^{2-}$, at potentials more positive than that for the oxidation of Cl^-, but these Ln^{4+} species are not stable on the time scale of voltammetry; therefore, they are difficult to characterize. The $^4G_{5/2}$, $^4G_{7/2} \leftarrow {}^4I_{9/2}$ transition for Nd^{3+} was split into several bands in the IL containing excess chloride, indicating that Nd^{3+} exists in a highly symmetrical octahedral environment. Although no hypersensitive transition is reported for Pr^{3+} in the range of wavelengths probed during this investigation, the increase in the intensity of the $^3P_0 \leftarrow {}^3H_4$ band that results from the complexation of Pr^{3+} in the IL containing excess Cl^-, but not in the neat IL, suggests that this band exhibits ligand-mediated pseudohypersensitivity. This phenomenon does not appear to have been observed before in ILs.

AUTHOR INFORMATION

Corresponding Author

*E-mail: chclh@chem1.olemiss.edu.

Notes

The authors declare no competing financial interest.

ACKNOWLEDGMENTS

This research was funded by the Division of Chemical Sciences, Geosciences, and Biosciences, Office of Basic Energy Science of the U.S. Department of Energy through Grant DE-AC02-98CH10886, Subcontract 154868, from Brookhaven National Laboratory.

REFERENCES

(1) Wilkes, J. S. *Green Chem.* **2002**, *4*, 73−80.
(2) Johnson, K. E. *Electrochem. Soc. Interface* **2007**, *16*, 38−41.
(3) Oldham, W. J.; Costa, D. A.; Smith, W. H. Development of room-temperature ionic liquids for applications in actinide chemistry. In *Ionic Liquids;* American Chemical Society: Washington, DC, 2002; Vol. *818*, pp 188−198.

(4) Venkatesan, K. A.; Rao, C. J.; Nagarajan, K.; Rao, P. R. V. *Int. J. Electrochem.* **2012**, *2012*, 12.
(5) Sun, X.; Luo, H.; Dai, S. *Chem. Rev.* **2012**, *112*, 2100−2128.
(6) Billard, I.; Ouadi, A.; Gaillard, C. *Anal. Bioanal. Chem.* **2011**, *400*, 1555−1566.
(7) Ha, S. H.; Menchavez, R. N.; Koo, Y.-M. *Korean J. Chem. Eng.* **2010**, *27*, 1360−1365.
(8) Cocalia, V. A.; Gutowski, K. E.; Rogers, R. D. *Coord. Chem. Rev.* **2006**, *250*, 755−764.
(9) Stockmann, T. J.; Ding, Z. *Anal. Chem.* **2011**, *83*, 7542−7549.
(10) Stockmann, T. J.; Lu, Y.; Zhang, J.; Girault, H. H.; Ding, Z. *Chem.—Eur. J.* **2011**, *17*, 13206−13216.
(11) Stockmann, T. J.; Montgomery, A.-M.; Ding, Z. *Anal. Chem.* **2012**, *84*, 6143−6149.
(12) Binnemans, K. *Chem. Rev.* **2007**, *107*, 2592−2614.
(13) Taubert, A. *Top. Curr. Chem.* **2009**, *290*, 127−159.
(14) Mudring, A.-V.; Tang, S. *Eur. J. Inorg. Chem.* **2010**, 2569−2581.
(15) Chou, L.-H.; Cleland, W. E.; Hussey, C. L. *Inorg. Chem.* **2012**, *51*, 11450−11457.
(16) Pan, Y.; Hussey, C. L. *Inorg. Chem.* **2013**, *52*, 3241−3252.
(17) Lipsztajn, M.; Osteryoung, R. A. *Inorg. Chem.* **1985**, *24*, 716−719.
(18) Castrillejo, Y.; Bermejo, M. R.; Diaz Arocas, P.; Martinez, A. M.; Barrado, E. *J. Electroanal. Chem.* **2005**, *579*, 343−358.
(19) Yamana, H.; Park, B. G.; Shirai, O.; Fujii, T.; Uehara, A.; Moriyama, H. *J. Alloys Compd.* **2006**, *408−412*, 66−70.
(20) Fukasawa, K.; Uehara, A.; Nagai, T.; Fujii, T.; Yamana, H. *J. Alloys Compd.* **2011**, *509*, 5112−5118.
(21) Fukasawa, K.; Uehara, A.; Nagai, T.; Fujii, T.; Yamana, H. *J. Nucl. Mater.* **2011**, *414*, 265−269.
(22) Fujii, T.; Nagai, T.; Sato, N.; Shira, O.; Yamana, H. *J. Alloys Compd.* **2005**, *393*, L1−L5.
(23) Mudring, A. V.; Babai, A.; Arenz, S.; Giernoth, R.; Binnemans, K.; Driesen, K.; Nockemann, P. *J. Alloys Compd.* **2006**, *418*, 204−208.
(24) Fujii, T.; Uehara, A.; Nagai, T.; Yamana, H. *Z. Naturforsch., A: Phys. Sci.* **2007**, *62*, 733−738.
(25) Greenwood, N. N.; Earnshaw, A. *Chemistry of the Elements;* Elsevier: Amsterdam, 2012; p 1341.
(26) Williams, D. B.; Stoll, M. E.; Scott, B. L.; Costa, D. A.; Oldham, W. J. *Chem. Commun.* **2005**, 1438−1440.
(27) Galliard, C.; Billard, I.; Chaumont, A.; Mekki, S.; Ouadi, A.; Denecke, M. A.; Moutiers, G.; Wipff, G. *Inorg. Chem.* **2005**, *44*, 8355−8367.
(28) Babai, A.; Mudring, A. V. *Dalton Trans.* **2006**, 1828−1830.
(29) Babai, A.; Mudring, A. V. *Chem. Mater.* **2005**, *17*, 6230−6238.
(30) Pan, Y.; Boyd, L. E.; Kruplak, J. F.; Cleland, W. E.; Wilkes, J. S.; Hussey, C. L. *J. Electrochem. Soc.* **2011**, *158*, F1−F9.
(31) Binnemans, K.; Görller-Walrand, C. *Chem. Phys. Lett.* **1995**, *235*, 163−174.
(32) Banks, C. V.; Klingman, D. W. *Anal. Chim. Acta* **1956**, *15*, 356−363.
(33) Gorller-Walrand, C.; Binnemans, K. Spectral intensities of f—f transitions. In *Handbook on the Chemistry and Physics of Rare Earths;* Gschneidner, K. A., Eyring, L., Eds.; Elsevier B.V.: Amsterdam, 1998; Vol. *25*, pp 101−264.
(34) Carnall, W. T. The Absorption and Fluorescence Spectra of Rare Earth Ions in Solution. In *Handbook on the Physics and Chemistry of Rare Earths;* Geschneider, K. A., Eyring, L., Eds.; North Holland: Amsterdam, 1979; Vol. *3*, pp 171−208.
(35) Moeller, T.; Brantley, J. C. *J. Am. Chem. Soc.* **1950**, *72*, 5447−5451.
(36) Driesen, K.; Nockemann, P.; Binnemans, K. *Chem. Phys. Lett.* **2004**, *395*, 306−310.
(37) Bhatt, A. I.; May, I.; Volkovich, V. A.; Collison, D.; Helliwell, M.; Polovov, I. B.; Lewin, R. G. *Inorg. Chem.* **2005**, *44*, 4934−4940.
(38) Yamagata, M.; Katayama, Y.; Miura, T. *J. Electrochem. Soc.* **2006**, *153*, E5−E9.
(39) Rao, C. J.; Venkatesan, K. A.; Nagaishi, R.; Srinivasan, T. G.; Rao, P. R. V. *Electrochim. Acta* **2009**, *54*, 4718−4725.
(40) Howlett, P. C.; Izgorodina, E. I.; Forsyth, M.; MacFarlane, D. R. *Z. Phys. Chem. (Muenchen, Ger.)* **2006**, *220*, 1483−1498.
(41) Howlett, P. C.; MacFarlane, D. R.; Hollenkamp, A. F. *Electrochem. Solid-State Lett.* **2004**, *7*, a97−A101.
(42) Forsyth, M.; Howlett, P. C.; Tan, S. K.; MacFarlane, D. R.; Birbilis, N. *Electrochem. Solid-State Lett.* **2006**, *9*, B52−B55.
(43) Howlett, P. C.; Brack, N.; Hollenkamp, A. F.; Forsyth, M.; MacFarlane, D. R. *J. Electrochem. Soc.* **2006**, *153*, A595−A606.
(44) Villagran, C.; Banks, C. E.; Deetlefs, M.; Driver, G.; Pitner, W. R.; Compton, R. G.; Hardacre, C. Chloride determination in ionic liquids. In *Ionic Liquids IIIb: Fundamentals, Progress, Challenges and Opportunities: Transformations and Processes;* American Chemical Society: Washington, DC, 2005; Vol. *902*, pp 244−258.
(45) Aldous, L.; Silvester, D. S.; Villagran, C.; Pitner, W. R.; Compton, R. G.; Lagunas, M. C.; Hardacre, C. *New J. Chem.* **2006**, *30*, 1576−1583.
(46) Singh, T. D.; Sumitra, C.; Yaiphaba, N.; Devi, H. D.; Devi, M. I.; Singh, N. R. *Spectrochim. Acta, Part A* **2005**, *61*, 1219−1225.
(47) Bendangsenla, N.; Moaienla, T.; Singh, T. D.; Sumitra, C.; Singh, N. R.; Devi, M. I. *Spectrochim. Acta, Part A* **2013**, *103*, 160−166.
(48) Laitinen, H. A.; Harris, W. E. *Chemical Analysis,* 2nd ed.; McGraw-Hill: New York, 1975.